Egypt. J. Chem. **Vol. 67**, No. 1 pp. 77 - 87 (2024)

Egyptian Journal of Chemistry

http://ejchem.journals.ekb.eg/

Efficient Ethanol Separation from Water Using Vacuum Membrane Distillation

R.M.Zarraa[1,2], Shaaban Nosier[3], A.A. Zatout[3], M. H. Abdel-Aziz[3,4],Mohammed S.Al-Geundi[2]

[1] *Petrochemical Engineering Department, Faculty of Engineering, Pharos University in Alexandria, Alexandria, Egypt.*

[2] *Chemical Engineering Department, Faculty of Engineering, Minia University, Minia, Egypt.*

[3] *Chemical Engineering Department, Faculty of Engineering, Alexandria University, Alexandria, Egypt.*

[4] *King Abdulaziz University, Chemical and Materials Engineering Department, Rabigh, Saudi Arabia.*

Abstract

This work presents an investigation into the efficiency of ethanol separation from water using vacuum membrane distillation (VMD). The study explores the influence of variables such as feed flow rate, initial ethanol concentration, and temperature on the performance of the distillation process. The polyvinylidene fluoride (PVDF) membrane was utilized due to its desirable properties such as high thermal stability, chemical resistance, and excellent mechanical properties. The results showed that the feed temperature had the greatest impact on the permeation flux. The permeate flux and ethanol flux increased with increasing initial ethanol concentration, while the separation factor decreased. Increasing the feed flow rate also resulted in increased permeate flux, ethanol flux, and separation factor. The study provides valuable insights into the optimization of the VMD process for efficient ethanol-water separation. The findings could potentially contribute to the development of more sustainable and efficient separation processes in the industry.

Keywords: Membrane distillation;PVDF ;separation; ethanol-water mixture; feed flow rate.

1. Introduction

In order to physically separate volatile components the thermally induced membrane distillation (MD) technique might be used [1]. MD often comes in four main types. : (1) sweeping gas membrane distillation (SGMD)[2] ; (2) direct contact membrane distillation (DCMD)[3] ;(3) air gap membrane distillation (AGMD) [3,4]; and (4) vacuum membrane distillation (VMD) [5–7]. Because VMD may achieve a higher percentage of rejection and larger flux than DCMD, it has been employed in separation processes like salt-water desalination. [8,9], volatile component separation [10], treatment of waste water [11–15]. the type of additives, the polymer's nature, its solvent and nonsolvent properties and synthesis method all affect the membrane's ability to prevent pore wetting and have a well-designed pore shape that will increase flux. Commercially. In the preparation of polymeric membranes for Membrane Distillation (MD) applications, a variety of solvents are utilized. These solvents, which are often classified as hazardous substances, pose environmental concerns due to their potential for harm. Some of the common solvents used in membrane preparation include N-methyl-2-pyrrolidone (NMP), dimethylformamide (DMF), dimethylacetamide (DMAc), and dimethyl sulfoxide (DMSO) as depicted in Table 1.[16–18]. N-methyl-2-pyrrolidone (NMP) is a popular solvent due to its high boiling point and excellent solvency for a wide range of polymers. However, it is classified as a reproductive toxin and is subject to stringent regulatory controls. Dimethylformamide (DMF) is another commonly used solvent, with a high dissolving power for a wide range of organic substances and polymers. However, it is also a hazardous substance, with potential health effects including liver damage and potential carcinogenic effects. Dimethylacetamide (DMAc) is a polar aprotic solvent with a high boiling point. It is used in the production of polyacrylic fibers and films. However, it is also a hazardous substance, with potential health effects including skin, eye, and respiratory irritation, and long-term exposure can lead to liver damage. Dimethyl sulfoxide (DMSO) is a less toxic alternative to the other solvents mentioned, with a lower environmental impact. It is a good solvent for a wide range of polar and non-polar

*Corresponding author e-mail: radwa.zarraa@pua.edu.eg

Receive Date: 05 August 2023 ,Revise Date: 22 August 2023, Accept Date: 28 August 2023

DOI: 10.21608/EJCHEM.2023.227328.8370

molecules and polymers. However, its relatively high cost compared to other solvents can be a limiting factor in its use.

While a variety of solvents can be used in the preparation of polymeric membranes for MD applications, each has its own set of advantages and disadvantages. The choice of solvent must therefore be made carefully, taking into account factors such as solvency power, toxicity, environmental impact, and cost.[19,20].

Table 1: Comparison of Solvents used for Membrane Preparation

Solvent	Surface tension (dyn/cm)	Viscosity (cP)	Vapor Pressure (mmHg)	Melting Point (°C)	Boiling Point (°C)	Hazards
Dimethylformamide (DMF)	48	0.97	13.4 (20 °C)	-97.5	153	Toxic, flammable, harmful to the environment
N-methyl-2-pyrrolidone (NMP)	47.9	0.95	10.1 (20 °C)	-63	202	Toxic, flammable, harmful to the environment
Dimethylacetamide (DMAc)	47.2	0.94	8.8 (20 °C)	-98	166	Toxic, flammable, harmful to the environment
Tetrahydrofuran (THF)	17.2	0.47	76.0 (20 °C)	-118	66	Flammable, harmful to the environment
Dimethyl sulfoxide (DMSO)	43.5	2	76.0 (20 °C)	-39	189	Toxic, corrosive, harmful to the environment
Acetone	23.7	0.32	234 (20 °C)	-95	56	Flammable, harmful to the environment
Ethyl acetate	24.5	0.47	200 (20 °C)	-84	77	Flammable, harmful to the environment

Relatively reduced energy costs than traditional distillation, reverse osmosis, and pervaporation are some of the main benefits of the membrane distillation process over conventional separation methods. Significantly less membrane fouling than with microfiltration, ultrafiltration, and reverse osmosis; a smaller vapor space than with traditional distillation; a significant rejection of dissolved, non-volatile species; operating temperature compared to traditional evaporation and lower operating pressure than pressure-driven membrane processes [21–25]. Other methods can be used in order to separate two components like Air-assisted liquid–liquid microextraction has which is used to extract a variety of analytes, including organic substances and medical analytes[26],liquid-liquid microextraction strategies based on the in-situ formation or in-situ decomposition of the deep eutectic solvent [27] as well as the air agitation which used as a green co-factor with dispersive liquid–liquid microextraction solidified floating organic drop , which addresses the major drawbacks of the previous techniques [28].Electrothermal atomic absorption spectrometry (ETAAS) could be used also especially in water treatment applications [29]

The study aims to provide a more efficient and cost-effective method for ethanol separation, which is important in various industries such as biofuel production and pharmaceuticals. The results of the study can contribute to the development of more sustainable and environmentally friendly separation processes.

2- Experimental part

The vacuum membrane distillation cell (VMDC) utilized in the current study, shown in Figure 1, the membrane cell made of two separate compartments made of acrylic polymeric material to prevent corrosion and to avoid the dissolving by the ethanol solution. The outer area of the cell is 54 m^2 and the polymeric PVDF membrane of 16 m^2 was inserted in the middle of cell between the two polymeric compartments. The polymeric membrane separates the cell into two chambers. The down part of cell contains two parts, one for entering the feed solution and the other part for which Leaving the retentate which recycled again to the feeding tank. The distance between the two parts was about 2cm.A vacuum using a vacuum pump was applied to other party cell (Upper party or permeate part) The permeate was obtained by condensing the fluxed vapor leaving the upper part of cell using Cold water that circulated through the condenser. The Condensed vapor (Permeate) leaving the condenser was collected in permeate tank.

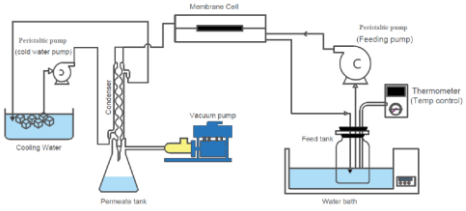

Fig 1. Schematic Representation of the Laboratory-Scale Vacuum Membrane Distillation Apparatus

Table 2: Main Characteristics of PVDF membrane

Membrane	Porosity	Contact angle	Pore size	Tensile strength	PH range
PVDF	45.6%	110°	0.22µm	4.5MPa	2-10

Different concentrations of the ethanol-water combination synthetic feed solution were made. namely 2, 5, 7 and 10 wt.% the temperature of feed solution was ranged for 20 to 60 ℃ and the volumetric flow rate of feed solution used in the present work were 0.064, 0.103, 0.143 and 0.179 L/min was adjusted by peristaltic pump. By measuring the amount of ethanol present in the aqueous solution gathered in the permeate tank, the amount of ethanol that passes through the membrane was found. Before each run, 2L of synthetics feed solution was placed in the feed tank and permitted to circulate through the cell membrane for one hour and a sample of permeate tank wasn't taken and analysed to obtain the concentration of ethanol. According to the next equation (1), The separation factor was calculated using the measured concentration:

$$\alpha_{Eth-H_2O} = \frac{\left(x_{Eth,P}/x_{w,P}\right)}{\left(x_{Eth,F}/x_{w,F}\right)} \quad (1)$$

The total permeates flux and ethanol permeate flux was determined by the following equations (2) and (3)

$$J_{tot} = \frac{w_p}{A \times t} \quad (2)$$

$$\mathrm{J_{Eth,t}} = \frac{\mathrm{w_{Eth,p}}}{\mathrm{A \times t}} \quad (3)$$

2. Membrane Preparation

Raw PVDF pellets (ρ = 1.78 g/m^3, average Mwt ≅275,000 g/mol) purchased from sigma Aldrich. The polymer (PVDF) was dried in a vacuum oven before membrane fabrication to get rid of any moisture. The PVDF membrane were prepared using a high-precision flat sheet membrane casting machine20 weight percent PVDF, 5 weight percent polyvinylpyrrolidone (PVP), and 75 weight percent N,N-dimethyl lactamide (DMAC) were combined to create the casting solution, it has been heated at 60 ℃ and stirred until the formation of a homogenous doping solution. A nonwoven fabric was used to support the membrane as the homogenous polymeric solution was cast onto a glass plate after being maintained in storage for 24 hours to allow for degassing. To eliminate the solvents, distilled water was added to a coagulation bath in which the casting glass plate was instantly submerged for 24 hours. The synthesized membrane was initially allowed to air dry for 48 hours at room temperature before being dried in a vacuum oven at 70 °C to eliminate the solvent and nonsolvent that had been confined within the membrane matrix

3. Characterization of the PVDF membranes

Scanning Electron Microscopy

The morphology of produced membranes was displayed using scanning electron microscopy (SEM). So as to achieve electrical conductivity, the membrane sample was layered with gold. A SEM TESCAN (3 XMU, MIRA) was used to scan the top surface of membranes to show the pores within them. [30]

Fourier Transform Infrared Spectroscopy (FTIR)

it is one of the most effective methods for sample characterization to determine the functional groups and the possible molecular bonds between chemical compounds. FTIR is used for quantitative and qualitative analysis and it is applicable for a varied range of materials and conditions. A spectrophotometer is a device responsible for the determination of the absorption spectrum of a sample. FTIR spectrophotometer (Bruker,Alpha) is much faster than the traditional spectrophotometer in providing the IR spectrum.[31]

Contact Angle

The contact angle governs the membrane surface's hydrophilicity and wetability. The contact angle was measured using a compact video microscope (CVM). The average drop volume was 10 l, and the contact time was 10 s. Each value was the average of 10 repeated measurements. The testing procedure is based on ASTM D5946-96 standard procedures for corona-treated polymer films employing measurements of the water contact angle and ASTM D724-99 standard test technique for the surface wet ability of paper. [32,33].

Membrane Porosity

The following equation, which uses density as a unit, can be utilized to determine the porosity of the membrane. After being submerged in isopropanol for six hours, the membrane was dried using tissue paper. Equation (4) was used to determine the porosity by measuring the weight of the wiped-and-dried membrane [34].

$$\mathrm{J_{Eth,t}} = \frac{(m_b/\rho_b)}{(m_b/\rho_b) + (m_b/\rho_b)} \quad (4)$$

Pore size

Using ImageJ software (LOCI, University of Wisconsin, Madison, WI, USA), the typical PVDF membrane pore size was determined.[35]

Results and Discussion –

Scanning Electron Microscopy

Figures 2a and 2b presents the SEM imaging of the PVDF membrane was investigated. The SEM imaging was performed at an accelerating voltage of 15 kV showed the porosity of the fabricated PVDF membrane.

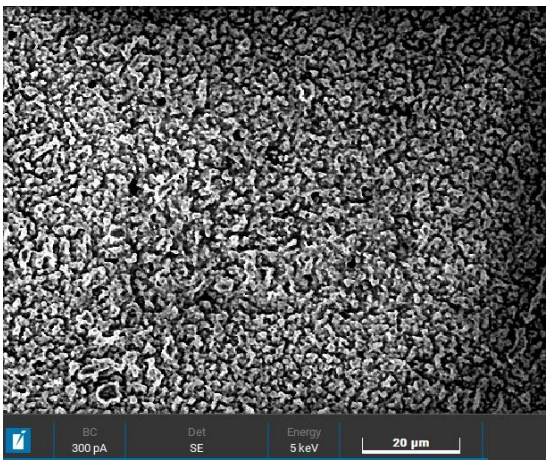

Fig 2a. Sem of PVDF membrane

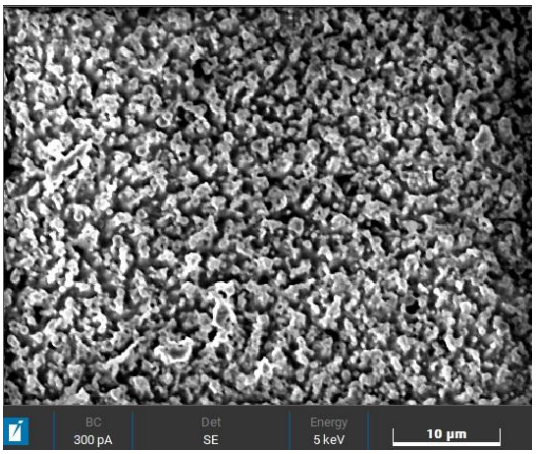

Fig 2b. Sem of PVDF membrane

Pore size, porosity and contact angle

The average pore size of 0.22 µm. Hydrophobicity of the membrane was analysed by the water contact angle test. In this experiment, the contact angle between the membrane sample and the deionized water was determined. and compared with that between methylene blue and membrane sample. The contact angle was carried out twice with different drop phases the contact angle between the $PVDF$ membrane and water drop phase is equal to (110°). To guarantee the accuracy of the results, the membrane porosity test was performed three times. By substituting in equation (4), it was discovered that it is equivalent to 45.6%. The primary membrane properties are outlined in Table 2.

Fourier Transform Infrared Spectrometer (FTIR)

The membrane's structure active bonds and phases are visible using a Fourier Transform Infrared Spectrometer (FTIR). As revealed in Figure 3, peaks at 3305,2948 cm^{-1} reveals the CH_2 asymmetric and symmetric stretching vibration, respectively. The peak at 1095 cm^{-1} is attributed to C-F wagging vibration, whereas those at 1406 and 870 cm^{-1} demonstrate CH_2 deformation and rocking vibrations, respectively. Additionally, distinctive bands at 1043, 1035, and 791 cm^{-1} are associated with the stretching, deformation, and bending vibrations of CF_2.

The presence of the Y-phase at 1241 and 433 cm^{-1} and the α-phase at 719 cm^{-1} are further characteristics of the PVDF membrane.

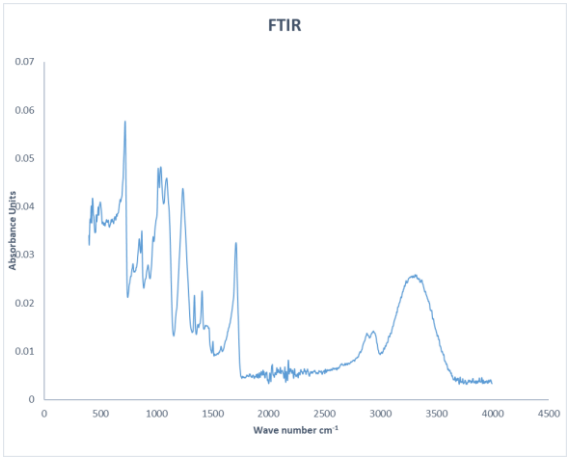

Fig 3. PVDF membrane FTIR

Figure (4) shows the outcome of the rate of volumetric flow on the total permeate flux at different initial ethanol concentration in the feed. It can be seen that; the total permeate flux was increased with the increase of the feed flow rate. This may be attributed to the followings:

Two resistances in series take place during the membrane separation

1. The barrier to mass transfer caused by the thickness of concentration boundary layer on the membrane feed side.
2. The resistance offers due to the membrane related to the first resistance, increasing the feed rate renders the concentration

boundary layer became thinner with a consequent increase the mass transfer coefficient and improve the mass transfer rate

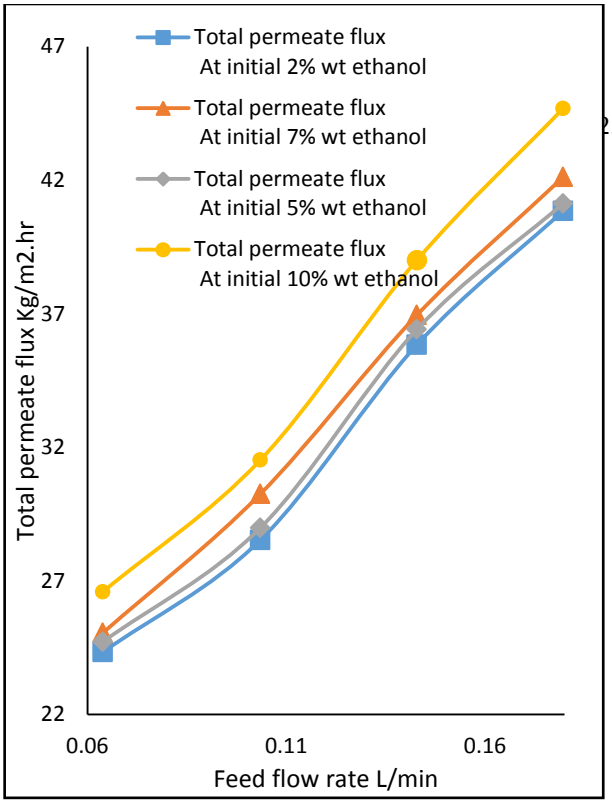

Fig 4.the outcome of volumetric flow rate on the total permeate flux at different initial ethanol concentration in the feed

On the other hand, at the membrane feed side, the mass transfer resistance is independent of flow rate and is linked to the membrane's properties for example its porosity, mean pore size, thickness, etc. Mass ethanol transport over the membrane may be aided by a higher the porosity of the membrane, bigger average pore size, and a thinner membrane thickness. With a lower flow rate, the water's convective mass transfer resistance may also predominate, and by raising the feed rate, the membrane flux may rise. However, a larger feed flow rate may cause more mass transfer resistance across the membrane, and an increase in feed velocity may not result in an increase in flux across the membrane. At temperature of 50 °C, as the feed flow rate raised from 0.064 L/min to 0.103 L/min, the permeate flux raised by about 68 % compared to that at flow rate 0.064 L/min at different initial ethanol concentrations.

Increasing the feed velocity, greater mixing in the membrane feed side produced owing to turbulence with consequent increase in the permeate flux.

At a temperature of 50 °C, Figure (5) illustrates the impact of feed flow rate on the total ethanol concentration. This was a scribed to

1. The hydrophobicity of membrane renders it highly selective to the ethanol than water.
2. At greater feed concentrations, Water is less volatile than ethanol. and produces less vapor. This enhanced the flow of ethanol across the membrane and exerted a significant partial vapor pressure on the membrane side of the feed.

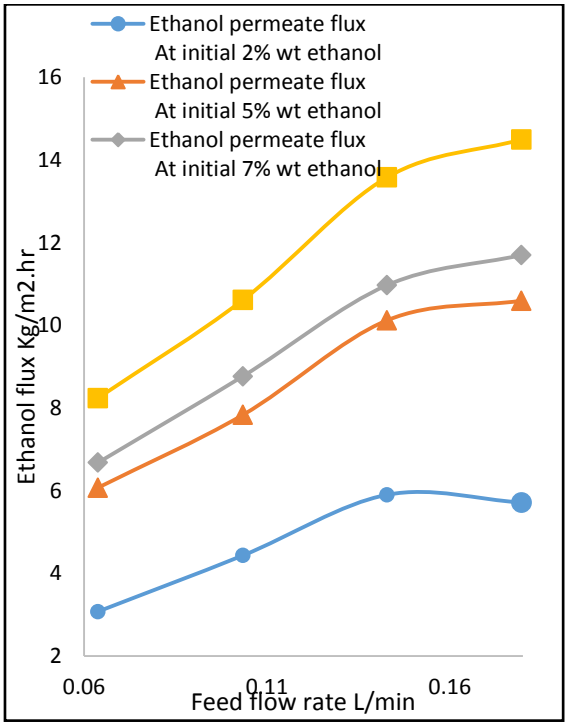

Fig 5.the effect of feed flow rate on the total ethanol concentration and at a temperature of 50 °C

At a temperature of 50 °C and various beginning concentrations of ethanol, Figure (6) illustrates the impact of feed flow rate on the separation factor. The separation factor increases with the feed flow rate from 0.064 L/min to 0.143 L/min and subsequently drops upon increasing the feed flow rate to 0.179 L/min.

At a specific feed flow rate, there is a decrease in the separation factor as the initial concentration of ethanol increases. This may be due to the fact that, as the concentration of ethanol increase, the viscosity of solution increases with consequent decrease in the mass transfer rate of total and ethanol permeate leading to decreasing the separation factor. The

relationship between the total permeate flux, the ethanol permeate flux, and the separation factor at various feed flow rates at a temperature of 50 °C is shown in Figures (7), (8), and (9) respectively. These findings demonstrated that when the ethanol percentage in the feed increases, the total permeate flux and ethanol flux both increase while the separation factor drops.

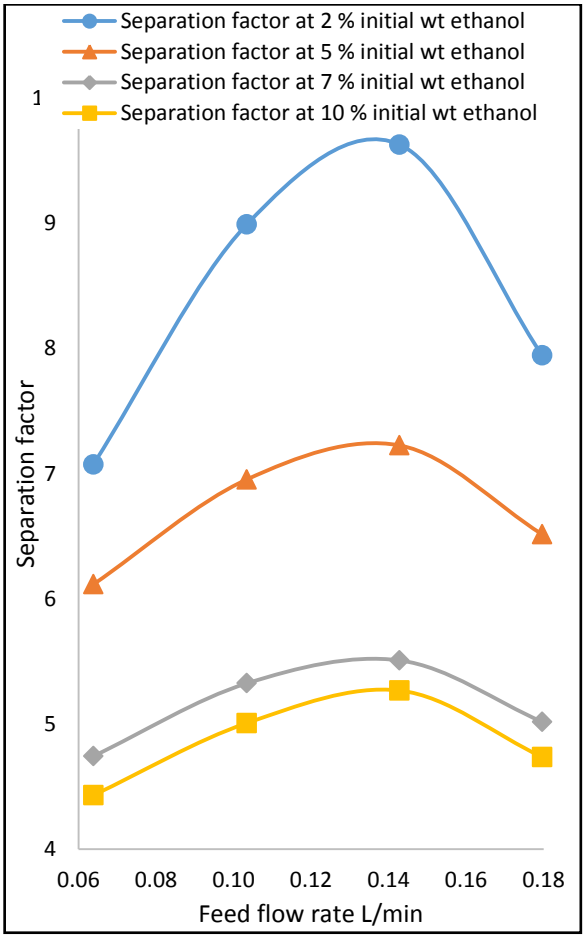

Fig 6.the effect of feed flow rate on the separation factor at a temperature of 50 °C and different initial concentration of ethanol

The effect of temperature was investigated by changing the feed temperature from 20 °C to 60 °C [36]with a step of 10 °C for one hour with a feed flow rate of 0.0103 $\frac{m^3}{min}$nitial concentration of ethanol of 2 wt%.

Total permeate flux, ethanol permeate flux, and separation factor increases with increasing the feed temperature as shown in figures 10, 11 and 12.

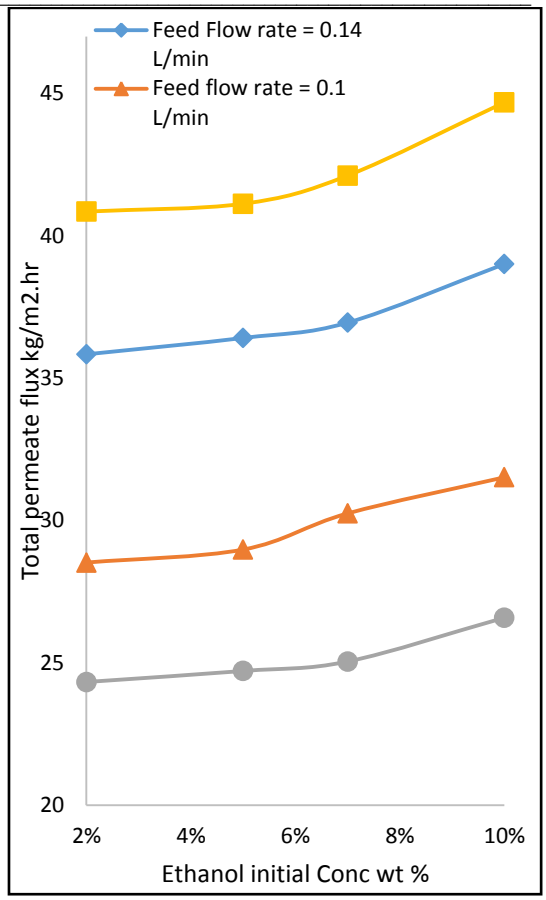

Fig 7. the impact of the initial ethanol concentration on the total permeate flux at various feed flow rates at 50 °C

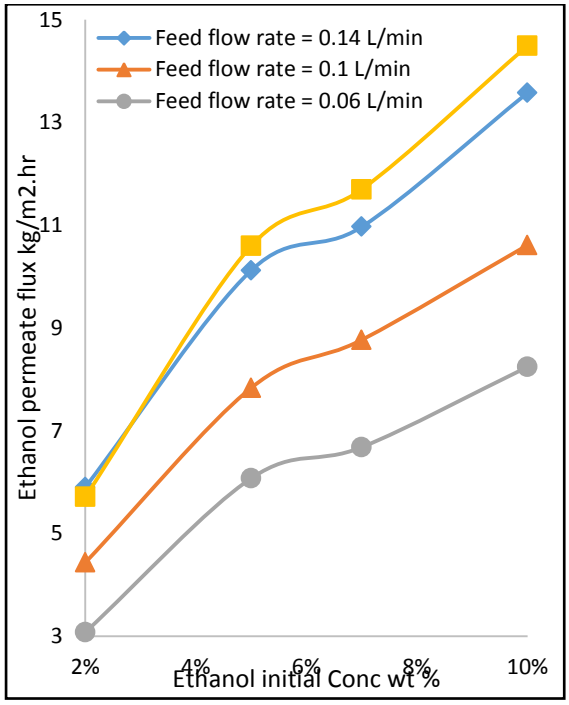

Fig 8. the impact of the ethanol's starting concentration on the ethanol permeate flux at various feed flow rates at a 50 °C

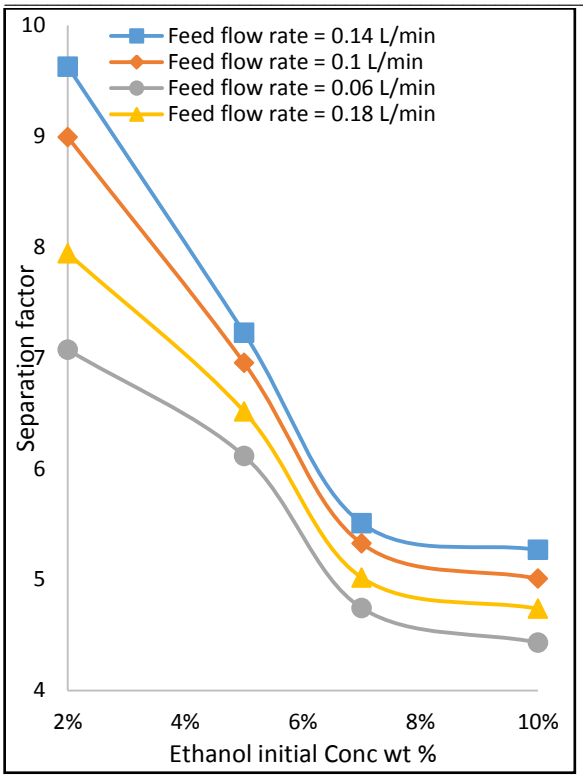

Fig 9. the impact of the initial ethanol content on the separation factor at various input flow rates at 50 °C

4- Conclusions

The study has successfully demonstrated the potential of vacuum membrane distillation (VMD) using a commercial polyvinylidene difluoride (PVDF) membrane for the separation of ethanol from a synthetic ethanol-water mixture. The experimental results showed that the feed temperature was the most significant factor affecting the permeation flux of the PVDF membrane.

The total permeate flux and ethanol flux were found to increase with the increasing initial ethanol concentration of the water-ethanol mixture, while the separation factor decreased. Furthermore, an increase in the feed flow rate led to an increase in the total permeate flux, ethanol flux, and separation factor.

However, the ethanol flux and separation factor decreased abruptly at temperatures above 50 °C, which can be attributed to the opposing effects of molecule size and component boiling point.

The study also highlighted the benefits of using dimethyl sulfoxide (DMSO) solvent for membrane synthesis. These findings provide valuable insights for the optimization of the VMD process and contribute to the development of more sustainable and efficient methods for the separation of volatile components from mixtures.

Further research is required to investigate the long-term stability of the PVDF membrane and the potential for scale-up of the VMD process for industrial applications. Additionally, the impact of other operating parameters, such as feed concentration and membrane thickness, on the performance of the VMD process should be explored.

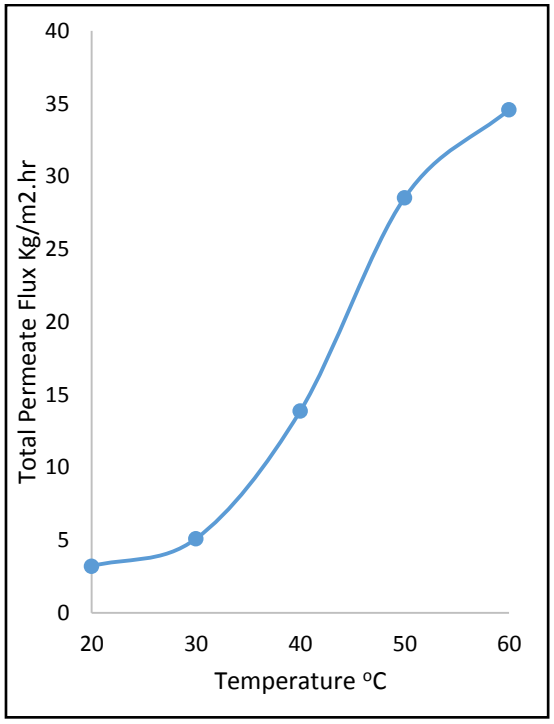

Fig 10. The temperature's impact on total permeate flux at 0.1 L/min feed rate and 2% starting ethanol concentration

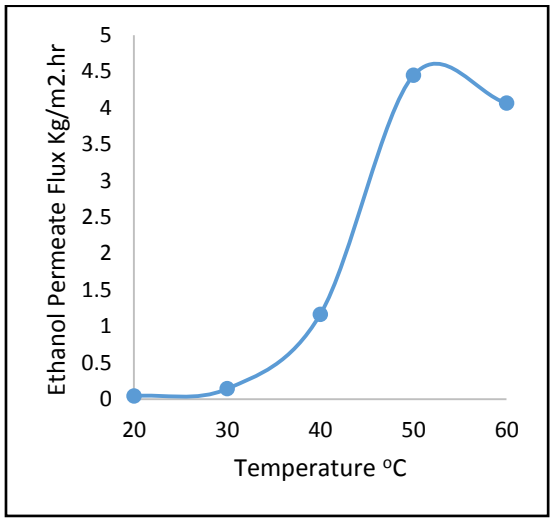

Fig 11. The impact of temperature on the ethanol permeate flux at 0.1 L/min and 2% wt starting ethanol concentration.

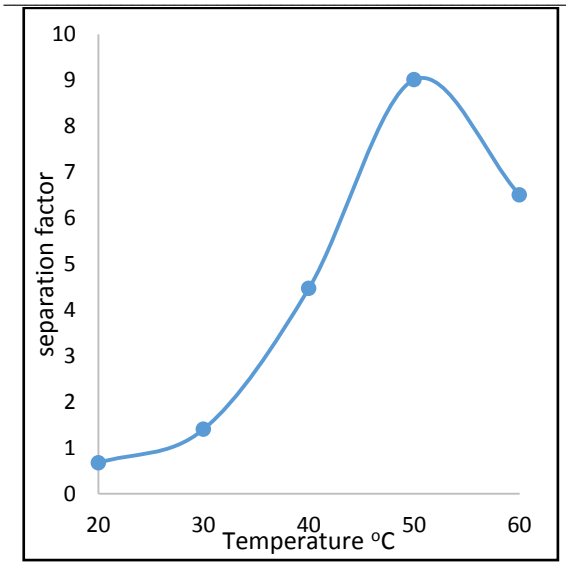

Fig 12. The impact of temperature on the separation factor at 0.1 L/min and 2% wt starting ethanol concentration.

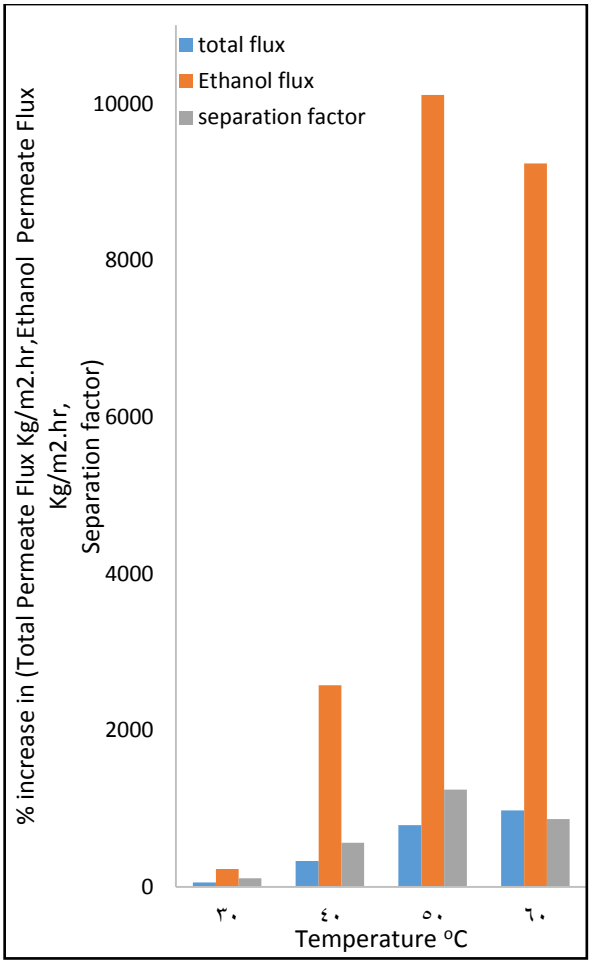

Figure 13 Effect of Feed Temperature on % increase at 20 °C, 2 % wt initial conc and 0.1 L/min flow rate

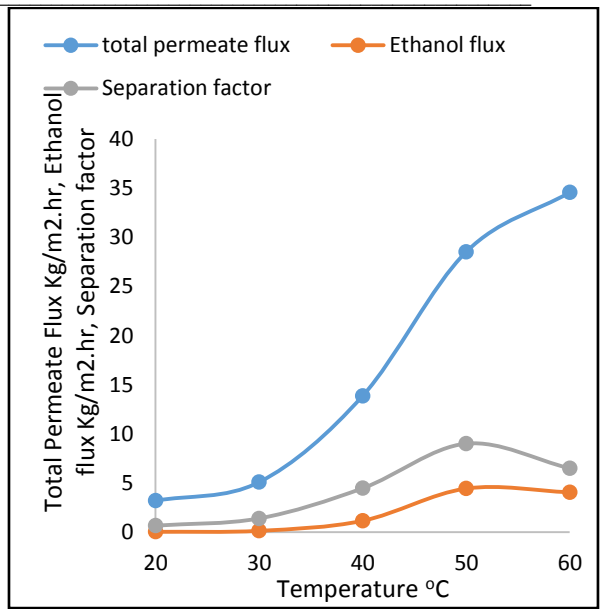

Figure 14 Effect of Feed Temperature on Total permeate flux, Ethanol flux and separation factor at 20 °C, 2 % wt initial conc and 0.1 L/min flow rate

Conflicts of interest

No conflicts need be reported.

Nomenclature

Symbol	Abbreviation and symbols
$\alpha_{Eth\text{-}H2O}$:	Separation factor or membrane selectivity
$x_{Eth,p}$:	Ethanol mole fraction in permeate.
$x_{Eth,F}$:	Initial ethanol mole fraction in the feed bulk liquid.
$x_{w,p}$	Water mole fraction in permeate.
$x_{w,F}$	Initial water mole fraction in the feed bulk liquid.
$J_{Eth,t}$	Total ethanol flux Kg/m^2.h
$W_{Eth,p}$	Accumulated mass of ethanol in permeate
J	Total Permeate flux Kg/m^2.h
W_p	Accumulated mass of permeate (Kg)
A	Effective membrane area 0.04*0.04=0.0016m^2
t	The operation of time (Hour)
ε	porosity of the membrane
m_p	mass of membrane (g)
m_b	mass of isopropanol absorbed (g)
ρ_p	Membrane's density (g/cm^3)
ρ_b	Isopropanol's density (g/cm^3)

References

[1] N.A.S. Muhamad, N.M. Mokhtar, R. Naim, W.J. Lau, A.F. Ismail, A Review of Membrane Distillation Process: Before, During and After Testing, Int. J. Eng. Technol. Sci. 6 (2019) 62–81. https://doi.org/10.15282/IJETS.V6I1.1549.

[2] M. Khayet, M.P. Godino, J.I. Mengual, Thermal boundary layers in sweeping gas

membrane distillation processes, AIChE J. 48 (2002) 1488–1497. https://doi.org/10.1002/AIC.690480713.

[3] C.J. Davey, P. Liu, F. Kamranvand, L. Williams, Y. Jiang, A. Parker, S. Tyrrel, E.J. McAdam, Membrane distillation for concentrated blackwater: Influence of configuration (air gap, direct contact, vacuum) on selectivity and water productivity, Sep. Purif. Technol. 263 (2021) 118390. https://doi.org/10.1016/J.SEPPUR.2021.118390.

[4] A.S. Alsaadi, N. Ghaffour, J.D. Li, S. Gray, L. Francis, H. Maab, G.L. Amy, Modeling of air-gap membrane distillation process: A theoretical and experimental study, J. Memb. Sci. 445 (2013) 53–65. https://doi.org/10.1016/J.MEMSCI.2013.05.049.

[5] R. Baghel, S. Upadhyaya, K. Singh, S.P. Chaurasia, A.B. Gupta, R.K. Dohare, A review on membrane applications and transport mechanisms in vacuum membrane distillation, Rev. Chem. Eng. 34 (2017) 73–106. https://doi.org/10.1515/REVCE-2016-0050/XML.

[6] R. Baghel, S. Upadhyaya, S.P. Chaurasia, K. Singh, S. Kalla, Optimization of process variables by the application of response surface methodology for naphthol blue black dye removal in vacuum membrane distillation, J. Clean. Prod. 199 (2018) 900–915. https://doi.org/10.1016/J.JCLEPRO.2018.07.214.

[7] R. Baghel, S. Kalla, S. Upadhyaya, S.P. Chaurasia, K. Singh, CFD modeling of vacuum membrane distillation for removal of Naphthol blue black dye from aqueous solution using COMSOL multiphysics, Chem. Eng. Res. Des. 158 (2020) 77–88. https://doi.org/10.1016/J.CHERD.2020.03.016.

[8] S. Upadhyaya, K. Singh, S.P. Chaurasia, R.K. Dohare, M. Agarwal, Mathematical and CFD modeling of vacuum membrane distillation for desalination, Desalin. Water Treat. 57 (2016) 11956–11971. https://doi.org/10.1080/19443994.2015.1048306.

[9] S. Upadhyaya, K. Singh, S.P. Chaurasia, R.K. Dohare, M. Agarwal, Recovery and development of correlations for heat and mass transfer in vacuum membrane distillation for desalination, New Pub Balaban. 57 (2016) 26886–26898. https://doi.org/10.1080/19443994.2016.1189245.

[10] V. Soni, J. Abildskov, G. Jonsson, R. Gani, Modeling and analysis of vacuum membrane distillation for the recovery of volatile aroma compounds from black currant juice, J. Memb. Sci. 320 (2008) 442–455. https://doi.org/10.1016/J.MEMSCI.2008.04.025.

[11] R. Baghel, S. Kalla, S. Upadhyaya, S. Chaurasia, J. Singh, Treatment of Sudan III Dye from wastewater using Vacuum Membrane Distillation, J. Basic Appl. Eng. Res. 4 (2017) 2350–2377.

[12] S. Gravelle, H. Yoshida, L. Joly, C. Ybert, L. Bocquet, Carbon membranes for efficient water-ethanol separation, J. Chem. Phys. 145 (2016). https://doi.org/10.1063/1.4963098/290922.

[13] M. Gryta, Effect of flow-rate on ethanol separation in membrane distillation process, Chem. Pap. 67 (2013) 1201–1209. https://doi.org/10.2478/S11696-013-0382-0/METRICS.

[14] S. Karimi, B. Ghobadian, G. Najafi, A. Nikian, R. Mamat, Effect of operating parameters on ethanol-water vacuum separation in an ethanol dehydration apparatus and process modeling with ANN, Chem. Prod. Process Model. 9 (2014) 179–191. https://doi.org/10.1515/CPPM-2014-0016.

[15] A. Rom, M. Strommer, A. Friedl, Comparison of sweepgas and vacuum membrane distillation as in-situ separation of ethanol from aqueous solutions, Chem. Eng. Trans. 39 (2014) 985–990. https://doi.org/10.3303/CET1439165.

[16] S. Tanaka, T. Iwata, M. Iji, Solvent effects on heterogeneous synthesis of cardanol-bonded cellulose thermoplastics, Polymer (Guildf). 99 (2016) 307–314. https://doi.org/10.1016/J.POLYMER.2016.07.024

[17] A. Figoli, T. Marino, S. Simone, E. Di Nicolò, X.M. Li, T. He, S. Tornaghi, E. Drioli, Towards non-toxic solvents for membrane preparation: A review, Green Chem. 16 (2014) 4034–4059. https://doi.org/10.1039/C4GC00613E.

[18] F. Russo, C. Ursino, E. Avruscio, G. Desiderio, A. Perrone, S. Santoro, F. Galiano, A. Figoli, Innovative Poly (Vinylidene Fluoride) (PVDF) Electrospun Nanofiber Membrane Preparation Using DMSO as a Low Toxicity Solvent, Membr. 2020, Vol. 10, Page 36. 10 (2020) 36. https://doi.org/10.3390/MEMBRANES10030036.

[19] N. Evenepoel, S. Wen, M. Tilahun Tsehaye, B. Van der Bruggen, Potential of DMSO as greener solvent for PES ultra- and nanofiltration membrane preparation, J. Appl. Polym. Sci. 135 (2018).

https://doi.org/10.1002/APP.46494.

[20] D. Matveev, V. Vasilevsky, V. Volkov, T. Plisko, A. Shustikov, A. Volkov, A. Bildyukevich, Fabrication of ultrafiltration membranes from non-toxic solvent dimethylsulfoxide: Benchmarking of commercially available acrylonitrile co-polymers, J. Environ. Chem. Eng. 10 (2022) 107061. https://doi.org/10.1016/J.JECE.2021.107061.

[21] L. Bazinet, C. Cossec, H. Gaudreau, Y. Desjardins, Production of a Phenolic Antioxidant Enriched Cranberry Juice by Electrodialysis with Filtration Membrane, J. Agric. Food Chem. 57 (2009) 10245–10251. https://doi.org/10.1021/JF9021114.

[22] D.S. Couto, M. Dornier, D. Pallet, M. Reynes, D. Dijoux, S.P. Freitas, L.M.C. Cabral, Evaluation of nanofi ltration membranes for the retention of anthocyanins of açai (euterpe oleracea mart.) juice, Desalin. Water Treat. 27 (2011) 108–113. https://doi.org/10.5004/DWT.2011.2067.

[23] F. dos Santos Gomes, P. Albuquerque da Costa, M.B. Domingues de Campos, S. Couri, L.M.C. Cabral, Concentration of watermelon juice by reverse osmosis process, Desalin. Water Treat. 27 (2011) 120–122. https://doi.org/10.5004/DWT.2011.2073.

[24] A.L. Quoc, M. Mondor, F. Lamarche, J. Makhlouf, Optimization of electrodialysis with bipolar membranes applied to cloudy apple juice: Minimization of malic acid and sugar losses, Innov. Food Sci. Emerg. Technol. 12 (2011) 45–49. https://doi.org/10.1016/J.IFSET.2010.12.007.

[25] I. Santana, P.D. Gurak, V.M. da Matta, S.P. Freitas, L.M.C. Cabral, Concentration of grape juice (vitis labrusca) by reverse osmosis process, Desalin. Water Treat. 27 (2011) 103–107. https://doi.org/10.5004/DWT.2011.2066.

[26] E.A. Azooz, H.S.A. Al-Wani, M.S. Gburi, E.H.B. Al-Muhanna, Recent modified air-assisted liquid-liquid microextraction applications for medicines and organic compounds in various samples: A review, Open Chem. 20 (2022) 525–540. https://doi.org/10.1515/CHEM-2022-0174/ASSET/GRAPHIC/J_CHEM-2022-0174_FIG_004.JPG.

[27] R. Ahmadi, E.A. Azooz, Y. Yamini, A.M. Ramezani, Liquid-liquid microextraction techniques based on in-situ formation/decomposition of deep eutectic solvents, TrAC Trends Anal. Chem. 161 (2023) 117019. https://doi.org/10.1016/J.TRAC.2023.117019.

[28] E.A. Azooz, M. Tuzen, W.I. Mortada, Green microextraction approach focuses on air-assisted dispersive liquid–liquid with solidified floating organic drop for preconcentration and determination of toxic metals in water and wastewater samples, Chem. Pap. 77 (2023) 3427–3438. https://doi.org/10.1007/S11696-023-02714-6/METRICS.

[29] D.J. Butcher, Recent advances in graphite furnace atomic absorption spectrometry: a review of fundamentals and applications, Https://Doi.Org/10.1080/05704928.2023.2192268. (2023). https://doi.org/10.1080/05704928.2023.2192268.

[30] M. Niamat, S. Sarfraz, E. Shehab, S.O. Ismail, Q.S. Khalid, Experimental Characterization of Electrical Discharge Machining of Aluminum 6061 T6 Alloy using Different Dielectrics, Arab. J. Sci. Eng. 44 (2019) 8043–8052. https://doi.org/10.1007/S13369-019-03987-4.

[31] M.A. Mohamed, J. Jaafar, A.F. Ismail, M.H.D. Othman, M.A. Rahman, Fourier Transform Infrared (FTIR) Spectroscopy, Membr. Charact. (2017) 3–29. https://doi.org/10.1016/B978-0-444-63776-5.00001-2.

[32] T. Huhtamäki, X. Tian, J.T. Korhonen, R.H.A. Ras, Surface-wetting characterization using contact-angle measurements, Nat. Protoc. 13 (2018) 1521–1538. https://doi.org/10.1038/S41596-018-0003-Z.

[33] M.H. Sorour, H.A. Hani, H.F. Shaalan, M. El-Toukhy, Fabrication and Characterization of Hydrophobic PVDF-based Hollow Fiber Membranes for Vacuum Membrane Distillation of Seawater and Desalination Brine, Egypt. J. Chem. 64 (2021) 4889–4899. https://doi.org/10.21608/EJCHEM.2021.68699.3500.

[34] X. Wang, L. Zhang, D. Sun, Q. An, H. Chen, Formation mechanism and crystallization of poly(vinylidene fluoride) membrane via immersion precipitation method, Desalination. 236 (2009) 170–178. https://doi.org/10.1016/J.DESAL.2007.10.064.

[35] A. Elrasheedy, M. Rabie, A. El-Shazly, M. Bassyouni, S.M.S. Abdel-Hamid, M.F. El Kady, Numerical Investigation of Fabricated MWCNTs/Polystyrene Nanofibrous Membrane for DCMD, Polym. 2021, Vol. 13, Page 160. 13 (2021) 160. https://doi.org/10.3390/POLYM13010160.

[36] A.R. Hussein, M.S. Gburi, N.M. Muslim,

E.A. Azooz, A greenness evaluation and environmental aspects of solidified floating organic drop microextraction for metals: A review, Trends Environ. Anal. Chem. 37 (2023) e00194. https://doi.org/10.1016/J.TEAC.2022.E00194.